Electron Transport in Single-Domain, Ferroelectric Barium Titanate

C. N. BERGLUND AND W. S. BAER
Bell Telephone Laboratories, Murray Hill, New Jersey
(Received 5 December 1966)

Conductivity, Hall-effect, and Seebeck-coefficient measurements on single-domain crystals of *n*-type $BaTiO_3$ are described. In the cubic phase above 126°C, the electron mobility is 0.5 cm^2/V sec. When the material becomes tetragonal, the mobility perpendicular to the *c* axis increases rapidly to 0.54 cm^2/V sec a few degrees below the transition temperature, then increases more slowly to 1.2 cm^2/V sec as the temperature decreases to 26°C. The mobility parallel to the *c* axis decreases rapidly to 0.35 cm^2/V sec a few degrees below the transition, then decreases slowly to 0.13 cm^2/V sec at 26°C. From the Seebeck-coefficient measurements, the density-of-states effective mass of cubic $BaTiO_3$ is $(6.5\pm2)m_0$. The experimental data in the tetragonal state are interpreted in terms of a relatively simple distortion of the band structure applicable to cubic perovskite-type semiconductors.

1. INTRODUCTION

ALTHOUGH much effort has gone into studying the electrical and optical properties of semiconducting barium titanate, relatively little is understood about electron transport in its ferroelectric state. Other cubic perovskite oxides such as $SrTiO_3$ [1] and $KTaO_3$ [2] exhibit conduction in bands formed from the transition-metal *d* orbitals. The very low electron mobilities of about 0.1 cm^2/V sec reported in tetragonal $BaTiO_3$ single crystals,[3] however, would imply that a Bloch band model for this material is marginal at best. Further, the infrared reflectivity in conducting, ferroelectric $BaTiO_3$ has been interpreted in terms of a small polaron, "hopping" model[4] rather than a band picture.

The difficulty of obtaining samples suitable for transport and optical experiments has been a principal barrier to $BaTiO_3$ research. Most electrical measurements have been made on reduced or doped ceramic samples, with particular emphasis placed on the positive temperature coefficient of resistance[5] (PTC) observed above 90°C. Few results are available for single crystals and, even with single crystals, experiments below the Curie temperature (~120°C) can be seriously affected by ferroelectric domain patterns. The transport measurements of Ikegami and Ueda[3] are thus difficult to interpret without knowing the domain structure of their single crystals. Mattes[6] has investigated the resistivity and piezoresistance in thin $BaTiO_3$ single crystals whose faces were perpendicular to the *c* axis in the tetragonal and orthorhombic phases. He concludes that a large anisotropy must exist between resistivities measured parallel and perpendicular to the *c* axis. Dichroism in the band-edge absorption in the tetragonal phase also has been reported by Casella and Keller.[7]

This paper discusses conductivity, Hall-effect, and Seebeck-coefficient measurements in single-domain, single-crystal $BaTiO_3$ in the cubic and tetragonal phases. Measurements both parallel and perpendicular to the tetragonal axis were made possible by the availability of large, pure, single crystals of $BaTiO_3$ from which single-domain samples could be obtained. It is shown that the transport properties of ferroelectric $BaTiO_3$ can be satisfactorily interpreted by a band model only slightly different from that assumed for the cubic perovskite compounds. Infrared and visible optical properties of these single-domain samples will be presented in a subsequent publication.

2. EXPERIMENTAL METHODS

The $BaTiO_3$ crystals studied were grown by Dr. A. Linz of M.I.T., and were cut into (100) slices approximately 1 mm thick. The samples were then reduced in flowing hydrogen. Uniformly reduced crystals with the largest single-domain regions were obtained by reduction at 900°–1000° for 8 h or more followed by a slow cooling to room temperature of several hours. All measurements were made on polished, single-domain parallelipipeds cut from the reduced slices.

The conductivity data were taken using the four-terminal method, separate measurements being made on each sample perpendicular to and parallel to the tetragonal *c* axis. Indium-gallium Ohmic contacts were made to the samples since it was found that evaporated chrome-gold contacts often tended to introduce internal strains into the $BaTiO_3$. The Hall measurements were made using standard techniques on rectangular samples of the order of $1\times2\times5$ mm.

Seebeck-coefficient measurements were made using an automatic technique.[8] Approximately square samples, typically $1\times3\times3$ mm, were mounted perpendicular to and parallel to the *c* axis on the heater assembly shown in Fig. 1 such that a one-dimensional temperature gradient could be set up. Care had to be taken that the samples were free to expand, since 90°

[1] H. R. P. Frederikse, W. R. Thurber, and W. R. Hosler, Phys. Rev. **134**, A442 (1964).
[2] S. H. Wemple, Phys. Rev. **137**, A1575 (1965).
[3] S. Ikegami and I. Ueda, J. Phys. Soc. Japan **19**, 159 (1964).
[4] P. Gerthsen, R. Groth, K. H. Hardtl, D. Heese, and H. G. Reik, Solid State Commun. **3**, 165 (1965).
[5] References to earlier work on the positive temperature coefficient of resistance are contained in J. B. MacChesney and J. F. Potter, J. Am. Ceram. Soc. **48**, 81 (1965).
[6] B. L. Mattes, J. Appl. Phys. **34**, 682 (1963).
[7] R. C. Casella and S. P. Keller, Phys. Rev. **116**, 1469 (1959).
[8] C. N. Berglund and R. C. Beairsto, Rev. Sci. Instr. **38**, 66 (1967).

domains were easily introduced into the samples by external stresses. Electrical and thermal contacts were made to the edges of the samples by the indium-gallium-mercury pools shown in Fig. 1. The two copper-constantan thermocouples were placed in the pools as near as possible to the edges of the $BaTiO_3$ samples. Careful experiments showed that such an arrangement introduced negligible error into the measurements.

The direction of the spontaneous polarization (the tetragonal c axis) was determined unambiguously by cutting a single-domain cube from one of the reduced samples and examining it between crossed polarizers. The direction of polarization established in this way was consistent both with the conductivity data of Mattes[6] and with the direction of the band-edge optical-absorption anisotropy reported by Casella and Keller.[7]

3. THEORETICAL MODEL

Kahn and Leyendecker[9] have proposed that the $SrTiO_3$ conduction band is siliconlike having six prolate ellipsoidal minima along the $\langle 100 \rangle$ directions at or near X_3, the Brillouin-zone edge [Fig. 2(a)]. Experimental data tend to support this model, not only in $SrTiO_3$,[10] but also in several other cubic perovskite-type semiconductors.[11] The $BaTiO_3$ transport properties to be described are also reasonably consistent with this model. However, more recent augmented-plane-wave (APW) band calculations suggest that the conduction-band minimum may be at Γ_{25}', the center of the Brillouin zone, as shown in Fig. 2(b).[12] The two possibilities are difficult to separate experimentally because both the band calculations and the experimental data to be presented suggest that the energy separation between X_3 and Γ_{25}' is only 0.1 to 0.15 eV. Thus the electrons contributing to the transport properties will be spread over a large region of k space in both cases, and similar transport behavior will result.

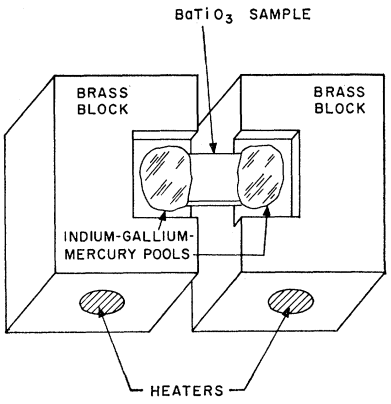

FIG. 1. Sample mount used for Seebeck-coefficient measurements on $BaTiO_3$.

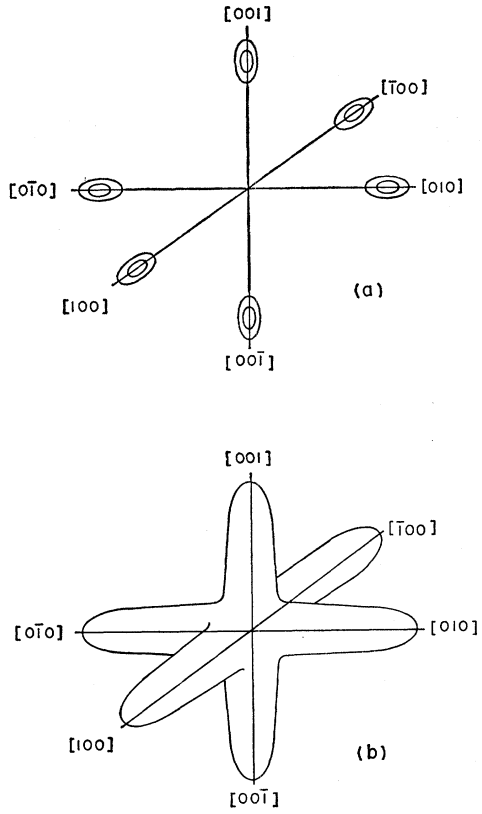

FIG. 2. (a) Constant-energy surfaces in the Brillouin zone near the conduction-band edge for conduction-band minima at X_3. (b) Constant-energy surface in the Brillouin zone near the conduction-band edge for conduction-band minimum at Γ_{25}'.

Since at present there is no unambiguous experimental evidence to decide which model is correct, the more familiar many-valley conduction-band model has been chosen for cubic $BaTiO_3$ as the basis on which to interpret the data. As a first approximation in the tetragonal state, it will be assumed that the conduction-band minima are the same as in the cubic state except for a simple shift in energy of the two minima lying along the tetragonal c axis with respect to the other four. It must also be assumed that no other conduction bands are near enough in energy to contribute to the conductivity. The experimental data to be presented indicate that one or more of the above assumptions is not completely accurate. However, the model does agree with the major features of the data and provides a simple basis on which to interpret the experimental results.

A. Conductivity and Hall Effect

The general expression for the isothermal current in the ith conduction-band minimum $j_\lambda^{(i)}$, in terms of

[9] A. H. Kahn and A. J. Leyendecker, Phys. Rev. **135**, A1351 (1964).

[10] H. P. R. Frederikse, W. R. Hosler, and W. R. Thurber, Phys. Rev. **143**, A648 (1966); J. F. Schooley, W. R. Hosler, and M. L. Cohen, Phys. Rev. Letters **12**, 474 (1964); M. L. Cohen, Phys. Rev. **134**, A511 (1964).

[11] I. Camlibel (private communication). Magnetoresistance measurements on $KTaO_3$ at 4.2°K are consistent with the many-valley model.

[12] L. F. Mattheiss (private communication).

applied electric and magnetic fields, is[13]

$$j_\lambda^{(i)}=\sigma_{\lambda\mu}^{(i)}E_\mu+\sigma_{\lambda\mu\gamma}^{(i)}E_\mu H_\gamma+\cdots, \quad (1)$$

where $\sigma_{\lambda\mu}^{(i)}$ and $\sigma_{\lambda\mu\gamma}^{(i)}$ are the conductivity and Hall conductivity tensors, respectively. When the $\langle 100\rangle$ axes of $BaTiO_3$ are chosen as the frame of reference, the symmetry of the conduction band makes the conductivity tensor diagonal with two independent components.

$$\sigma_l^{(i)}=n^{(i)}q^2\langle\tau\rangle/m_l^*$$

and

$$\sigma_t^{(i)}=n^{(i)}q^2\langle\tau\rangle/m_t^*, \quad (2)$$

where $\langle\tau\rangle$ is the average electron scattering time (assumed to be isotropic), $n^{(i)}$ is the density of electrons in the ith minimum, the subscript l refers to a direction along the $\langle 100\rangle$ axis on which the minimum is located, and the subscript t refers to a direction perpendicular to the $\langle 100\rangle$ axis. Similarly, the Hall conductivity tensor has two components, $\sigma_{Hl}^{(i)}$ when the magnetic field vector is parallel to the $\langle 100\rangle$ axis on which the minimum is located, and $\sigma_{Ht}^{(i)}$ when the magnetic field is perpendicular to the $\langle 100\rangle$ axis.

$$\sigma_{Hl}^{(i)}=n^{(i)}q^3\langle\tau^2\rangle/cm_t^{*2}, \quad \sigma_{Ht}^{(i)}=n^{(i)}q^3\langle\tau^2\rangle/cm_l^*m_t^*, \quad (3)$$

where $\langle\tau^2\rangle$ is the average of the square of the electron scattering time.

The total mobility and Hall coefficient are found by suitable summations of Eqs. (2) and (3) over all six conduction-band minima. In the cubic state, the summations are relatively simple and lead to an isotropic conductivity

$$\sigma_0=\tfrac{1}{3}(Nq^2\langle\tau\rangle)[(1/m_l^*)+(2/m_t^*)], \quad (4)$$

where N is the donor density. (It has been assumed that the donors are fully ionized and the sample is nondegenerate.) If longitudinal and transverse valley mobilities are defined

$$\mu_l=q\langle\tau\rangle/m_l^* \quad \text{and} \quad \mu_t=q\langle\tau\rangle/m_t^*, \quad (5)$$

Eq. (4) gives for the mobility in the cubic state

$$\mu_0=\sigma_0/qN=\tfrac{1}{3}\mu_l+\tfrac{2}{3}\mu_t. \quad (6)$$

The Hall coefficient R is the sum of the six Hall conductivities divided by the square of the total conductivity. Hence, in the cubic state

$$R=\frac{\langle\tau^2\rangle}{Nqc\langle\tau\rangle^2}\frac{[1/3m_t^{*2}+2/3m_t^*m_l^*]}{[1/3m_l^*+2/3m_t^*]^2}. \quad (7)$$

When $BaTiO_3$ becomes tetragonal (point group C_{4V}), it can be shown to have two independent mobilities, $\mu_\perp$ perpendicular to and $\mu_{||}$ parallel to the tetragonal c axis, and two independent Hall coefficients, $R_\perp$ when the magnetic field is perpendicular to and $R_{||}$ when the magnetic field is parallel to the tetragonal c axis. If we assume that the two minima along the c axis move in energy with respect to the other four by an amount ΔE (assumed positive if the c-axis minima move down), the population ratio in the valleys is given by the Boltzmann factor $\exp(\Delta E/kT)$, and the measured mobilities can be written

$$\mu_{||}=\sigma_{||}/qN=(\mu_l+2\mu_te^{-\Delta E/kT})/(1+2e^{-\Delta E/kT}) \quad (8)$$

and

$$\mu_\perp=\sigma_\perp/qN=[\mu_t+e^{-\Delta E/kT}(\mu_l+\mu_t)]/(1+2e^{-\Delta E/kT}). \quad (9)$$

Defining η as the valley mobility ratio μ_l/μ_t, and a as $e^{-\Delta E/kT}$, Eqs. (8) and (9) become

$$\mu_{||}=\mu_t(\eta+2a)/(1+2a), \quad (10)$$

$$\mu_\perp=\mu_t[1+a(1+\eta)]/(1+2a), \quad (11)$$

and

$$\frac{\mu_\perp}{\mu_{||}}=\frac{[1+a(1+\eta)]}{[\eta+2a]}. \quad (12)$$

Similarly

$$R_{||}=\frac{\langle\tau^2\rangle}{Nqc\langle\tau\rangle^2}\frac{(1+2a)(1+2\eta a)}{[1+a(1+\eta)]^2} \quad (13)$$

and

$$R_\perp=\frac{\langle\tau^2\rangle}{Nqc\langle\tau\rangle^2}\frac{[\eta+a(1+\eta)](1+2a)}{[1+a(1+\eta)](\eta+2a)}. \quad (14)$$

It should be noted that Eqs. (8) through (14) were derived assuming that the valley mobilities at a given temperature are independent of the degree of tetragonality. This implies the additional assumption that intervalley scattering is relatively weak.

Herring and Vogt[14] have shown that the relaxation time τ is not in general isotropic as assumed above. However, inclusion of an anisotropic relaxation time does not aid in the interpretation of the data, and in view of the previous simplifying assumptions of the model provides an unnecessary complication in the equations.

B. Seebeck Coefficient

It has been shown that if there are two types of carriers in a semiconductor contributing to the conductivity, and if these two carriers have partial Seebeck coefficients S_1 and S_2, the Seebeck coefficient of the semiconductor S is given by[15]

$$S=(\sigma_1/\sigma_0)S_1+(\sigma_2/\sigma_0)S_2, \quad (15)$$

where σ_1 and σ_2 are the contributions to the total conductivity σ_0 of the two types of carriers. This concept can be extended to a many-valleyed conduction band of a semiconductor such as $BaTiO_3$, where each valley has a unique Seebeck coefficient and contributes a certain fraction to the total conductivity. If the Seebeck

[13] C. Herring, Bell System Tech. J. **34**, 237 (1965).

[14] C. Herring and E. Vogt, Phys. Rev. **101**, 944 (1956).

[15] See, for instance, A. H. Wilson, *The Theory of Metals* (Cambridge University Press, Cambridge, England, 1953), p. 205.

coefficient of the two minima located along the c axis is S_c and the Seebeck coefficient of the other four minima is S_a, then the quantities defined in Sec. 3 A can be used to show that

$$S_{\parallel}=(\eta S_c+2aS_a)/(\eta+2a), \quad (16)$$

$$S_{\perp}=[S_c+aS_a(1+\eta)]/[1+a(1+\eta)], \quad (17)$$

where $S_{\parallel}$ is the Seebeck coefficient measured parallel to and $S_{\perp}$ is the Seebeck coefficient measured perpendicular to the tetragonal c axis. In Eqs. (15), (16), and (17), the Seebeck coefficients S_1, S_2, S_a, and S_c are isotropic. The anisotropy indicated by Eqs. (16) and (17) in the measured Seebeck coefficients arises from the anisotropic conductivities used in the summation of Eq. (15).

For a nondegenerate conduction-band minimum the Seebeck coefficient is

$$S=(k/q)[(-E_F/kT)+\beta], \quad (18)$$

where E_F is the Fermi energy relative to the conduction-band minimum, and β is a constant which depends on the energy dependence of the electron-scattering mechanisms (between 2 and 3 for lattice scattering). Equation (18) is strictly correct only if the electron energy dependence of the scattering is isotropic. In this case, the Seebeck coefficient in Eq. (18) will be isotropic. However, even if the electron energy dependence of the scattering is not isotropic, Eq. (18) is expected to be a good approximation. Here it will be assumed that Eq. (18) applies for $BaTiO_3$ and that β at a given temperature is the same for all six conduction-band minima. (A discussion of the validity of these assumptions will be given later.) Hence, the difference between the two Seebeck coefficients S_c and S_a is

$$S_c-S_a=(k/q)(\Delta E/kT), \quad (19)$$

and substituting Eq. (19) in Eqs. (16) and (17)

$$S_{\perp}-S_{\parallel}=\frac{a\Delta E}{qT}\left(\frac{2}{\eta+2a}-\frac{(1+\eta)}{1+a(1+\eta)}\right). \quad (20)$$

At a given temperature, Eqs. (12) and (20) indicate that measurements of $\mu_{\parallel}$, $\mu_{\perp}$, $S_{\parallel}$, and $S_{\perp}$ give sufficient information to determine μ_l, μ_t, and ΔE. A comparison of experimental data from $BaTiO_3$ with Eqs. (12) and (20) as a function of temperature, particularly through the tetragonal to cubic transition, will then be an indication of the validity of the proposed model.

4. EXPERIMENTAL RESULTS

A. Conductivity and Hall Effect

The conductivity parallel to and perpendicular to the c axis was measured on several single-domain $BaTiO_3$ samples from 26 to 150°C. All samples gave essentially the same results, the conductivity perpendicular to the c axis being larger than that parallel to the c axis.

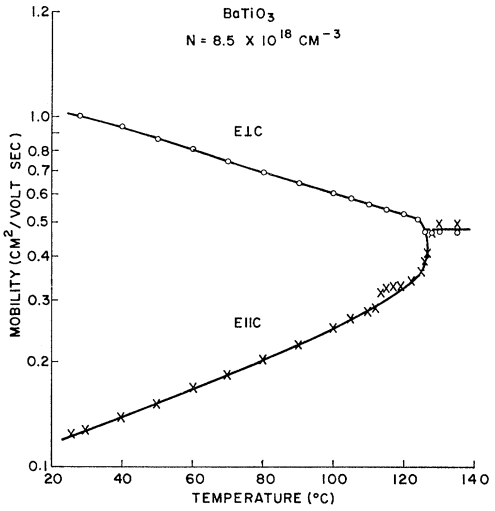

FIG. 3. Typical temperature dependence of the electron mobility in $BaTiO_3$.

Figure 3 shows typical data. The curves have been normalized to give mobility by dividing by the temperature-independent free-carrier charge density qN determined from subsequent Hall measurements. The magnitude of qN was obtained assuming the Hall mobility to be equal to the drift mobility in the cubic phase. This assumption is probably reasonable in view of experimental results on other similar perovskites.[2]

In the $E \parallel c$ curve, a 90° domain formed in the sample leading to the peculiarity in the data near 115°C. The solid line shows the usual behavior as determined from subsequent measurements where no domains formed. Within a few degrees of the transition, the two mobilities are shown as rapidly varying functions of temperature, but not discontinuous as expected. It is believed that this is due to small temperature gradients which existed in the samples during measurements. Above the ferroelectric transition temperature of 126°C up to a temperature of 150°C, the mobility appears to be nearly temperature-independent.

Hall data were obtained from several samples with $H \parallel c$ and $H \perp c$, but with current flowing perpendicular to the c axis in both cases. Although this gave measurements of both $R_{\parallel}$ and $R_{\perp}$, only the conductivity perpendicular to the c axis was obtained during the Hall measurements. Most of the samples measured had carrier concentrations between 10^{18} and 10^{19} cm^{-3} and the Hall voltages were relatively small. Typical data are shown in Fig. 4(a). The accuracy of the Hall-coefficient measurements on these samples is no better than ±20%. Although this accuracy is not sufficient to allow detection of the small variations in R expected from the η- and a-dependent terms in Eqs. (13) and (14), it can be concluded that the mobility is essentially independent of carrier concentration and that the Hall coefficient is constant within experimental error over the temperature range from 26 to 200°C.

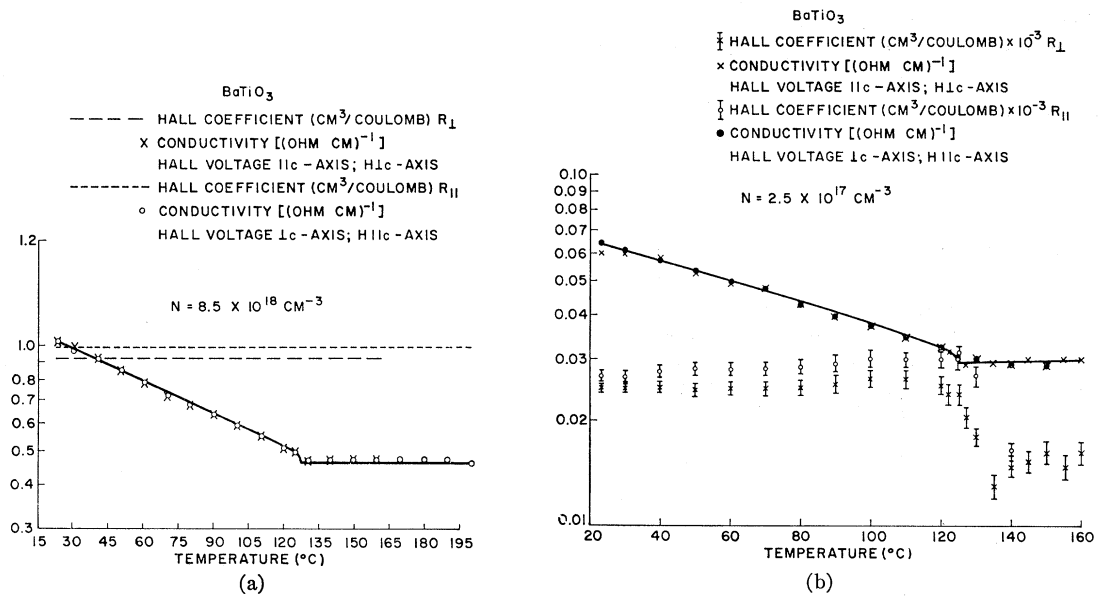

FIG. 4. (a) Typical Hall data for $BaTiO_3$. Both Hall coefficients are shown as constants, since within the experimental error of $\pm 20\%$ there was no detectable temperature dependence. (b) Hall data for a lightly-doped $BaTiO_3$ sample.

The latter conclusion supports the earlier assumption that the donors in $BaTiO_3$ are fully ionized over the temperature range of study.

One sample that was studied had a relatively low carrier concentration of 2.5×10^{17} cm^{-3}, resulting in considerably higher Hall voltages and better accuracy. This sample exhibited electron mobilities similar to those obtained from the more heavily-doped samples and a rapid variation in both Hall coefficients near the ferroelectric transition temperature. The temperature dependence of the Hall coefficients is shown in Fig. 4(b). The effects could not be unambiguously reproduced on any more heavily doped samples, and no samples with carrier concentrations below 2.5×10^{17} cm^{-3} were available.

The Hall and conductivity data shown in Figs. 3 and 4 and the Seebeck-coefficient measurements to be described later are plotted using temperature as the variable. However, the electrical properties of $BaTiO_3$ are in general related to temperature in a very complicated way because of the tetragonality. More easily interpreted comparisons of the experimental results to the proposed theoretical model can be made if a different variable is used. The directly measured mobility ratio $\mu_\perp/\mu_{||}$ has been found to be a convenient variable which is easily related to theory.

If μ_0 is defined as the (isotropic) mobility in the cubic state, then Eqs. (10), (11), and (12) can be manipulated to show that

$$\frac{\mu_{||}}{\mu_0}=\frac{3}{1+2\mu_\perp/\mu_{||}}\frac{\mu_{tt}}{\mu_{tc}} \tag{21}$$

and

$$\frac{\mu_\perp}{\mu_0}=\frac{3\mu_\perp/\mu_{||}}{1+2\mu_\perp/\mu_{||}}\frac{\mu_{tt}}{\mu_{tc}}, \tag{22}$$

where μ_{tt} and μ_{tc} are the transverse valley mobilities in the tetragonal and cubic states, respectively. If it is assumed that the valley mobilities suffer no discontinuity in going through the ferroelectric transition and do not change with temperature, then the factor μ_{tt}/μ_{tc} can be set equal to unity. Hence, a plot of $\mu_{||}/\mu_0$ and $\mu_\perp/\mu_0$ versus $\mu_\perp/\mu_{||}$ compared to Eqs. (21) and (22) with μ_{tt}/μ_{tc} set equal to unity provides an excellent test of the theoretical model since the shapes of the curves depend only on the assumption of six equivalent minima in the $\langle 100\rangle$ directions. In addition, it should be possible to determine if there is a discontinuity in the valley mobilities at the ferroelectric transition and to determine the temperature dependence of the valley mobilities. Figure 5 shows the experimental points obtained from Fig. 3 and the theoretical curves obtained from Eqs. (21) and (22). Points corresponding to values of $\mu_\perp/\mu_{||}$ less than 1.3 are not shown because their accuracy will be seriously affected by small temperature gradients in the sample. For $\mu_\perp/\mu_{||}$ less than 3 (corresponding to temperatures greater than 90°C), there is excellent agreement between the theoretical curves and experimental points. In fact, by varying the ratio μ_{tt}/μ_{tc} for best fit over this temperature range, it could be concluded that μ_{tt}/μ_{tc} is unity within an estimated error of 5%. However, for $\mu_\perp/\mu_{||}$ greater than 3, there is a departure of the experimental points from the theory. Although this departure may be partially due to a simple temperature dependence of the valley mobilities, it will be shown later that the major cause of the discrepancy is a breakdown of one or more of the assumptions on which the theoretical model is based.

One important result of the data in Fig. 5 is that there is no evidence of any discontinuity in the valley

mobilities at the ferroelectric transition temperature. If there is a discontinuity, it must be less than 5%.

Figure 4 shows Hall data for both $H \parallel c$ and $H \perp c$. Since the high carrier densities of the samples studied limited the accuracy of the measurements, a plot of $R_{\parallel}$ and $R_{\perp}$ from Fig. 4 versus the mobility ratio $\mu_{\perp}/\mu_{\parallel}$ cannot be unambiguously analyzed on the basis of Eqs. (13) and (14). However, using the values of η and a established from the Seebeck measurements, it can be shown that the ratio of $R_{\parallel}/R_{\perp}$ should vary within the range from 0.75 to 1.1 over the temperature range studied. Results similar to those shown in Fig. 4(b) are expected, with a rapid change occurring in the vicinity of the ferroelectric transition. These expected variations in R are within the accuracy of the measurements shown in Fig. 4(a).

B. Seebeck Coefficient

Figure 6 shows typical measurements of the Seebeck coefficient of $BaTiO_3$ from room temperature to 160°C on a sample containing 6.0×10^{18} cm^{-3} free electrons. The relative accuracy of each curve (parallel to and perpendicular to the c axis) is better than 1%. It was noted on most samples that the curves for the two measurements did not match as expected at temperatures above the ferroelectric transition. Careful measurements, after demounting and remounting the samples several times, showed that the same relative temperature variation of the Seebeck coefficient was always measured, but the curves after demounting and remounting usually differed by a temperature-independent scale factor which varied over ±5%. It was concluded that the problem was due to difficulties in electrically contacting the small samples at the same points as the temperature was measured. This would cause the values of Seebeck coefficient to be in error

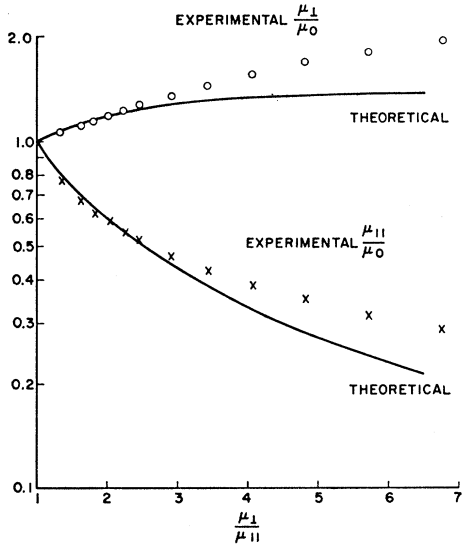

FIG. 5. Mobilities of $BaTiO_3$ normalized to the cubic phase mobility plotted versus the mobility anisotropy.

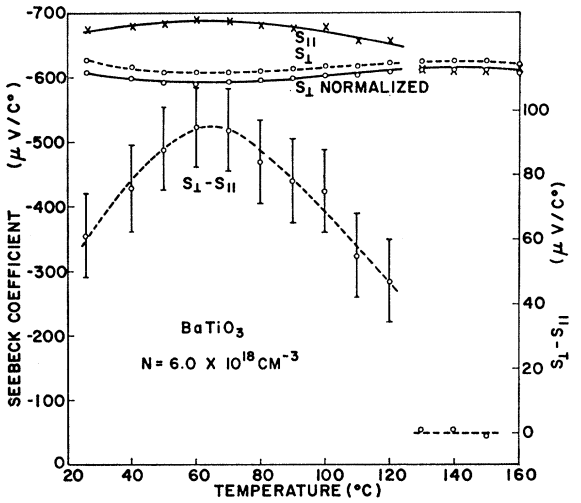

FIG. 6. Seebeck-coefficient data for a typical sample of $BaTiO_3$.

in an absolute sense, but would not significantly affect the relative accuracy or temperature dependence of the measurements. For this reason, the $S_\perp$ curve in Fig. 6 has been arbitrarily normalized to $S_\parallel$ at temperatures above the ferroelectric transition where $S_\parallel$ should equal $S_\perp$. Such a procedure assures that the error in the quantity of major interest, the difference between $S_\parallel$ and $S_\perp$, will be minimized. The temperature dependence of $S_\perp - S_\parallel$ using the normalized $S_\perp$ curve is also shown in Fig. 6. The error margin was estimated assuming an accuracy in $S_\perp$ and $S_\parallel$ of ±1%. As a result, it may be too pessimistic.

All $BaTiO_3$ samples measured exhibited behavior similar to that shown in Fig. 6, although there were minor differences. The Seebeck coefficient parallel to the c axis $S_\parallel$ was always more negative than $S_\perp$ in the tetragonal state, and the difference in the two Seebeck coefficients, $S_\perp - S_\parallel$, always reached a maximum of approximately 100 μV/°C near 60 to 70°C independent of carrier concentration within experimental error.

The Seebeck coefficient can be used with Eq. (18) to provide an estimate of the conduction-band effective mass. Assuming the primary electron-scattering mechanism is by lattice vibrations, β in Eq. (18) lies between 2 and 3 and the conduction-band effective mass of $BaTiO_3$ in the cubic state is $(6.5\pm2)m_0$, where m_0 is the free-electron mass. This value compares with $0.8m_0$ for $KTaO_3$ [2] and $5m_0$ for $SrTiO_3$.[16]

More detailed information on the nature of the conduction-band minima in $BaTiO_3$ can be obtained by examining the experimental data shown in Figs. 5 and 6 using Eqs. (10), (11), (12), and (20). Figure 7 shows the theoretical difference in Seebeck coefficient, $S_\perp - S_\parallel$, based on the theoretical model, with the

[16] H. P. R. Frederikse and G. A. Candela, Phys. Rev. **147**, 583 (1966).

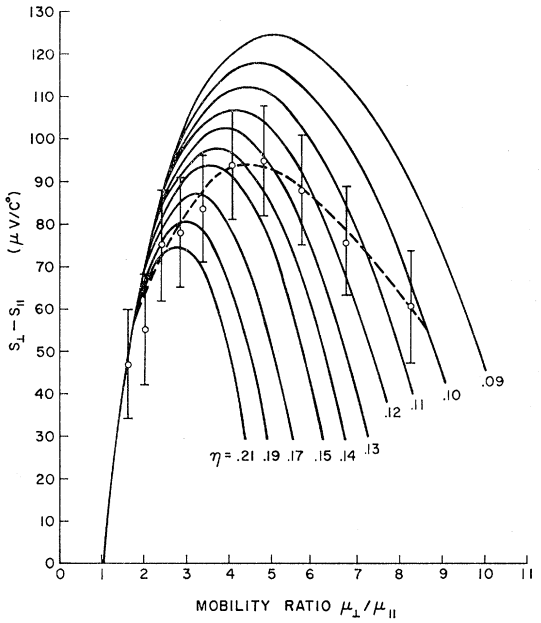

FIG. 7. Seebeck-coefficient anisotropy versus the mobility anisotropy.

mobility ratio $\mu_\perp/\mu_{||}$ as the parameter. Also shown are the experimental points from Fig. 6.

Although there is reasonable agreement in shape and magnitude between the theoretical and experimental results, η must be allowed to vary from 0.10 ± 0.01 at 26°C to 0.18 ± 0.04 near the transition temperature (126°C) to explain the data. This result suggests that one or more of the assumptions on which the theoretical model is based are not accurate over the entire temperature range studied. However, the fact that very close agreement between theory and experiment was obtained for $\mu_\perp/\mu_{||}$ less than 3 (temperatures above approximately 90°C) seems sufficient to verify the basic assumptions of the nature of the conduction band in $BaTiO_3$ in the cubic phase. In addition, it can be concluded that the transverse valley mobility μ_t is approximately five times greater than the longitudinal valley mobility μ_l in the cubic phase, and that the c-axis minima move to lower energy with respect to the other four when the semiconductor becomes tetragonal.

It has been pointed out that η must be allowed to change from 0.10 at 26°C to approximately 0.18 at the transition temperature in order to explain the experimental results using the simple theoretical model. These values of η apply primarily to the c-axis minima, since they make the dominant contributions to the conductivity in the tetragonal phase. Equations (10), (11), (12), and (20) also indicate that this change in η results almost entirely from a change in the transverse valley mobility μ_t. Over the temperature range studied, μ_l remains nearly constant at approximately 0.13 cm²/V sec, while μ_t varies from 1.2 cm²/V sec at 26°C to 0.65 cm²/V sec at the ferroelectric transition.

Figure 8 shows the energy separation between the c-axis minima and the a-axis minima as a function of temperature calculated from the experimental data using Eqs. (10), (11), (12), and (20). The curve at temperatures below 90°C is dotted to emphasize the fact that the experimental results do not accurately match the theoretical model with constant η in this range. The c-axis minima move down with respect to the four a-axis minima approximately 0.020 eV at the ferroelectric transition, and as temperature is lowered the energy separation increases rapidly to nearly 0.120 eV at room temperature. Although the energy separation varies with temperature similar to the square of the spontaneous polarization, the agreement is not sufficiently good to allow unambiguous conclusions to be drawn.

5. DISCUSSION OF RESULTS

The experimental data indicate that a siliconlike conduction band with ellipsoidal minima along the ⟨100⟩ directions at or near X_3 is a reasonable first approximation for $BaTiO_3$. On the basis of this model, the minima are prolate, with approximately a five to one ratio between the transverse and longitudinal mobilities in the cubic state. Assuming that the electron relaxation time is isotropic, the Seebeck measurements indicate that the transverse effective mass is approximately $1.5m_0$ and the longitudinal effective mass is approximately $7.5m_0$ if the conduction-band minima are within the Brillouin zone. If the conduction-band minima are at X_3, the transverse mass is approximately $1.0m_0$ and the longitudinal mass is approximately $5.0m_0$.

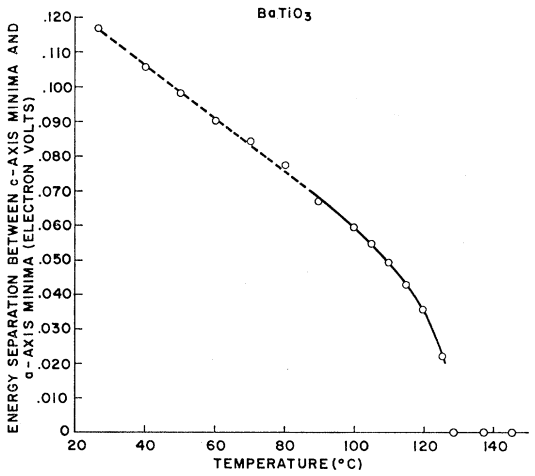

FIG. 8. Calculated energy separation between the c-axis conduction-band minima and the a-axis conduction-band minima as a function of temperature for $BaTiO_3$.

If the cosine approximation is used for the conduction band between Γ_{25}' and X_3, the previously determined longitudinal effective mass can be used to show that the energy separation between Γ_{25}' and X_3 is approximately 0.15 eV. However, it was found from the measurements that the two c-axis conduction-band minima move down in energy with respect to the other four minima approximately 0.02 eV at the ferroelectric transition, increasing to nearly 0.12 eV at 26°C. Hence, the energy separation between the minima is comparable to the energy separation between Γ_{25}' and X_3. This suggests that there is some distortion in the shape of the conduction band and a non-negligible change in the valley effective masses with temperature. Since the theoretical model used to interpret the data assumed constant effective masses at all temperatures, this fact may have partially caused the departure from theoretical expectations noted in the experiments.

In the analysis of the Seebeck coefficient no detailed knowledge of the band structure and electron-scattering mechanisms were available. As a result, two basic assumptions were required. The electron energy dependence of the scattering in each conduction-band minimum must be isotropic, and the value of the scattering term β must be the same for all six minima at each temperature. Both assumptions are probably reasonable in the cubic state provided that the electron-scattering mechanism is primarily by lattice modes. In the tetragonal state the band distortions discussed above, and any significant intervalley scattering, will tend to break down both assumptions leading to a departure from the theoretical model as the tetragonality increases. However, it is not expected that significant errors will result since β in Eq. (18) is relatively insensitive to both effects. The breakdown of the assumptions leading to Eqs. (10), (11), (12), (13), and (14) will be a much larger source of error.

It has been proposed that the major electron-scattering mechanism in several perovskite-type semiconductors is by the transverse optical (ferroelectric) mode.[17] However, there is no evidence that this mode is dominant in the scattering of electrons in $BaTiO_3$. The frequency of the transverse optical vibrations decreases to near zero as the temperature is decreased to the ferroelectric transition temperature. At the ferroelectric transition temperature, it is expected that a discontinuous increase in its frequency would occur which would in general result in discontinuous increases in the longitudinal and transverse valley mobilities. However, the experimental data show that the mobility is only weakly temperature-dependent above the ferroelectric transition temperature, and the valley mobilities undergo no noticeable discontinuity at the tetragonal phase transition.

[17] S. H. Wemple, A. Jayaraman, and M. Di Domenico, Jr., Phys. Rev. Letters **17**, 142 (1966).

It has previously been suggested that the conduction-band minimum in $BaTiO_3$ may be at Γ_{25}' rather than at or near X_3. The analysis of the data on this model is rather complex, but to a first approximation the results would be basically the same as the many-valleyed model. The very small energy separation between Γ_{25}' and X_3 makes it difficult experimentally to separate the two possibilities. In both cases, electrons contributing to the conductivity will not be restricted to values of k very near the conduction-band minima over the temperature range of study. It is interesting to note, however, that the experimental departure from the simple many-valleyed model arises primarily from a temperature dependence in the transverse valley mobility μ_t. The longitudinal valley mobility μ_l remains essentially constant from 26°C to beyond the transition temperature of 126°C.

6. CONCLUSIONS

The transport measurements on single-domain crystals of $BaTiO_3$ confirm Mattes's result that there is a large conductivity anisotropy in the tetragonal state. The electron mobility is approximately 0.5 cm^2/V sec in the cubic state near the Curie temperature, with the mobility perpendicular to the c axis increasing to 1.2 cm^2/V sec and parallel to the c axis decreasing to 0.13 cm^2/V sec as the temperature is decreased to 26°C. These values are slightly smaller than those reported for $SrTiO_3$. The dominant electron-scattering mechanism was not evident from the experimental results. However, the data near the ferroelectric transition indicate that scattering by the transverse optical (ferroelectric) mode may not be important in $BaTiO_3$.

The transport properties of $BaTiO_3$ can be satisfactorily described if the conduction band is many-valleyed having six prolate ellipsoidal minima along the $\langle 100 \rangle$ directions (near X_3). Using this model, the two minima lying along the c axis move down in energy with respect to the other four 0.02 eV at the ferroelectric transition temperature increasing to 0.12 eV at 26°C. The longitudinal to transverse mass ratio in each valley is approximately 5:1 in the cubic state, with the transverse mass estimated to be $1.0m_0$ to $1.5m_0$ depending on the location of the conduction-band minima in the Brillouin zone. The density-of-states effective mass is estimated from the Seebeck-coefficient measurements to be $6.5m_0$, slightly larger than that of $SrTiO_3$.

Although the many-valleyed model described above is in good agreement with the experimental results, a model in which the conduction-band minimum is at the center of the Brillouin zone (Γ_{25}') must also be considered. The data can also be described if the conduction-band minimum is at $k=0$ with constant-energy surfaces consisting of long "fingers" extending along the $\langle 100 \rangle$ directions. For both models, the energy separation between Γ_{25}' and X_3 is approximately 0.15 eV.

Hence, it is difficult to determine unambiguously which model is applicable for $BaTiO_3$.

ACKNOWLEDGMENTS

The authors would like to express their sincere appreciation to R. Griffith and R. C. Beairsto for reducing and preparing the $BaTiO_3$ samples and assisting with the measurements; to R. Wolfe for helpful discussions and suggestions on the Seebeck-coefficient measurements and interpretation; to G. E. Smith and D. Kahng for helpful suggestions and comments on the work; to L. F. Mattheiss for making available the results of his energy-band calculations prior to publication; and to C. Herring for critical reading of the manuscript.

PHYSICAL REVIEW VOLUME 157, NUMBER 2 10 MAY 1967

Volume-Dependent Exchange and the Heisenberg Ferromagnet

R. H. DONALDSON
Department of Physics, Monash University, Victoria, Australia
(Received 28 December 1966)

The Weiss molecular-field treatment of the Heisenberg model of ferromagnetism has been extended by the introduction of volume-dependent exchange interactions. An interaction of this type produces a contribution to the expansion coefficient. This paper presents computed results for the temperature dependence of the specific heat (including the simple Weiss model with constant exchange), the magnetization, and the expansion coefficient. The application to antiferromagnetic MnF_2 is discussed.

1. INTRODUCTION

THE standard Weiss molecular-field model of ferromagnetism and antiferromagnetism[1] deals with the Hamiltonian

$$\mathcal{H}=-2J_0\sum_{i>j}\mathbf{S}_i\cdot\mathbf{S}_j,$$

where J_0, the nearest-neighbor exchange interaction, is a temperature-independent constant. In real solids, the strength of the exchange interaction will be influenced by changes in the separation of the interacting moments, and if the lattice is deformable the thermal and magnetic properties of the ordered state can be considerably modified.[2] In particular, the variation of the magnetization from maximum alignment at $T=0°K$ to zero at the transition temperature T_0 will be accompanied by changes in the lattice volume; i.e., the effect of the volume-dependent exchange interaction is to produce a contribution to the expansion coefficient. Bean and Rodbell[2] showed that if the interaction is sufficiently strong, the transition from the ordered state to the paramagnetic state can become first order.

However, in this paper the discussion is restricted to evaluation of the properties of the Heisenberg ferromagnet and antiferromagnet (with volume-dependent exchange) where the transition is of the usual second-order type. The molecular-field approximation is made throughout. The expansion coefficient has been calculated on this model, and has the form observed experimentally.[3,4] Another effect which is reported here is the influence of this type of interaction on the magnetic contribution to the specific heat. Volume-dependent exchange results in an increase in the total energy E associated with the magnetic specific heat;

$$E=\int_0^{T_0}C dT.$$

According to the simple molecular-field model, the value of E/NkT_0 is independent of the magnitude of J and has the value $\frac{3}{2}S(S+1)$, where S is the spin per atom and N is the total number of magnetic atoms in the specimen.[5] A model which includes volume-dependent exchange interaction predicts an increase in the value of E by as much as 20% above the value predicted by the simple molecular-field model. This arises from the modified temperature dependence of the magnetic specific heat (discussed in Sec. 5). The interaction results in an increase in the specific-heat discontinuity at the transition temperature, the size of the discontinuity increasing monotonically with the increase in $\partial J/\partial V$.

Calculations have been made of the temperature dependence of the magnetization, the magnetic specific heats, and the expansion coefficients for various magnitudes of the interaction. Results have been computed also for the magnetic specific heat associated with the standard molecular-field model where the exchange

[1] J. S. Smart, *Effective Field Theories of Magnetism* (W. B. Saunders Company, Philadelphia, 1966), p. 22.
[2] C. P. Bean and D. S. Rodbell, Phys. Rev. **126**, 104 (1962).
[3] M. Foex, Compt. Rend. **227**, 193 (1948).
[4] D. F. Gibbons, Phys. Rev. **115**, 1194 (1959).
[5] J. A. Hofmann, A. Paskin, K. J. Tauer, and R. J. Weiss, J. Phys. Chem. Solids **1**, 45 (1956).